



OPEN ACCESS

EDITED BY
Dong Liu,
Guangzhou Institute of Chemistry (CAS),
China

REVIEWED BY
Jining Li,
Nanjing Normal University, China
Yingqun Ma,
Chinese Research Academy of
Environmental Sciences, China
Zheng Wang,
Nanjing Forestry University, China
Xiaoguang Xu,
Nanjing Normal University, China

*CORRESPONDENCE
Chaonan Han,
✉ hcn_125@163.com

SPECIALTY SECTION
This article was submitted to
Biogeoscience,
a section of the journal
Frontiers in Earth Science

RECEIVED 14 November 2022
ACCEPTED 20 December 2022
PUBLISHED 04 January 2023

CITATION
Han C, Tang Y, Wu H, Sun N, Dai Y and
Dai T (2023), Periodic variations of
phosphorus migration and transformation
in a eutrophic lake of China: The role of
algae bloom and collapse.
Front. Earth Sci. 10:1097679.
doi: 10.3389/feart.2022.1097679

COPYRIGHT
© 2023 Han, Tang, Wu, Sun, Dai and Dai.
This is an open-access article distributed
under the terms of the [Creative Commons
Attribution License \(CC BY\)](https://creativecommons.org/licenses/by/4.0/). The use,
distribution or reproduction in other
forums is permitted, provided the original
author(s) and the copyright owner(s) are
credited and that the original publication in
this journal is cited, in accordance with
accepted academic practice. No use,
distribution or reproduction is permitted
which does not comply with these terms.

Periodic variations of phosphorus migration and transformation in a eutrophic lake of China: The role of algae bloom and collapse

Chaonan Han*, Yu Tang, Hao Wu, Ningning Sun, Yan Dai and Tianhao Dai

School of Civil Engineering, Nanjing Forestry University, Nanjing, China

It is a two-way interaction between algae bloom events and nutrient cycles in aquatic environments. In Meiliang bay of Taihu Lake, phosphorus (P) forms in the water, sediment and pore water, and bacterial community structures in the sediment were investigated in June 2021 (the algae bloom period) and December 2021 (the algae collapse period). The aim of this study is to clarify the periodic variations of P migration and transformation driven by algae bloom and collapse. Results showed that concentrations of total P and total particulate P in the water during the algae bloom period (.13–.25 mg/L) were much higher than those during the algae collapse period (0–.13 mg/L), which was mainly caused by the uptake of phosphate (PO_4^{3-}) by algae in the surface water. Compared with the algae bloom period, there were higher concentrations of organic P (OP), iron-bound P (FeP) and inorganic P in the sediments during the algae collapse period. The proportions of OP and FeP in total P in the sediments increased from 19% to 17% during the algae bloom period to 27% and 33% during the algae collapse period. These suggest the cumulative trend of OP and FeP in the sediments during the algae collapse period, and FeP might be formed through the processes of OP mineralization and P adsorption by iron oxides/hydroxides in the sediments. Different routes of sediment P regeneration existed over the two periods. During the algae bloom period, the similar vertical variations of labile PO_4^{3-} and labile Fe^{2+} in the sediments provided *in situ*, high-resolution evidence for FeP reductive dissolution driven by FRBs activities. During the algae collapse period, OP mineralization driven by organic P-solubilizing bacteria activities and accelerated by the sulfate reduction process was confirmed by the similar vertical variations of labile PO_4^{3-} and labile S^{2-} in the sediments. Therefore, treatment approaches and management practices should consider the periodic variations of internal P cycles in aquatic environments during the algae bloom and algae collapse periods to avoid inefficient treatments of lake eutrophication and algae bloom.

KEYWORDS

phosphorus, migration and transformation, bacteria community, algae bloom, eutrophic lakes

1 Introduction

Lake eutrophication and harmful algae blooms have developed worldwide in recent decades, which seriously affected freshwater ecosystems, water supply securities and human livelihoods (Gilbert, 2017; Kouakou and Poder, 2019). Phosphorus (P) is an essential nutrient element for living organisms and is considered the limiting factor in freshwater eutrophication (Schelske, 2009). One primary cause of lake eutrophication is excess P input, particularly the

input of dissolved phosphate (PO_4^{3-}) which is more available to algae growth and reproduction (Glibert and Burford, 2017). Thus, reducing exogenous P input has been a common management strategy for eutrophication prevention and control (Schindler et al., 2016). When exogenous P loadings were largely reduced, internal P release in aquatic environments can play important roles in developing algae blooms sequentially (Jeppesen et al., 2005; Lepori and Roberts, 2017). It was reported that internal P accumulation and release can be promoted by the influences associated with the algae bloom and algae decomposition processes (Han et al., 2015). The growth and reproduction of algae assimilates a lot of dissolved P from water and converts it to intracellular P, which is accumulated in sediments through the sedimentation of dead algae cells (Schelske, 2009). The intracellular P of algae is dominant in the form of organic P, which is potentially bioavailable and is easily decomposed by microorganisms (Zhang et al., 2017; Yuan et al., 2020).

Beyond that, there are lots of other P forms such as inorganic P and iron-bound P in sediments, which could also be transformed under suitable biogeochemical conditions (Gu S. et al., 2019; Wang et al., 2020). Iron cycle played an important role in the mobility of P in sediments through the processes of P adsorption by iron oxides/hydroxides and iron oxides/hydroxides reductive dissolution (Chen et al., 2015; Gao et al., 2016). (Chen et al., 2018) indicated that algae decomposition by microorganisms exhausted oxygen resulting in the anoxia condition, which accelerated the reduction of iron oxides/hydroxides in sediments. In the anoxia and reductive sediments, sulfate reduction may be coupled with iron oxides/hydroxides reduction, affecting sediment P regeneration (Ma et al., 2017). Therefore, P migration and transformation in the water and sediments isn't only driven by algae life activities, but also associated with iron and sulfur cycles especially in sediments.

A complete process of an algae bloom event mainly contains two distinct periods, the algae bloom period and the algae collapse period. Over the two periods, algae activities can also affect the microbial communities in aquatic environments, which indirectly affected the migration and transformation of P (Qian et al., 2011). Zhang et al. (Zhang et al., 2021) indicated that the abundance of the dominant bacterial communities in the sediments and overlying water changed significantly during the degradation processes of *Cladophora oligoclora*. (Fan et al., 2018) found that there were different bacterial communities in the sediments of the cyanobacteria-dominant zone and the macrophyte-dominated zone of Taihu lake, which resulted in the different mechanisms of ferric iron reduction and P availability in the sediments. In addition, P-solubilizing bacteria can also promote sediment P release, particularly taking part in OP degradation (Liu et al., 2017). (Tu et al., 2022) indicated that Proteobacteria and Actinobacteriota were the predominant phyla among P-solubilizing bacteria during the cyanobacterial resuscitation phase. However, there remains a lack of explanation of the periodic variations of P forms in the sediments from the perspective of microbial community variations during the algae bloom period and algae collapse period.

Taihu Lake is the third largest freshwater lake in China. It is a shallow lake with an average water depth of 1.9 m. Due to water eutrophication, Taihu Lake has experienced large-scale cyanobacteria blooms since the 1990s, especially occurred in the northern and western areas (Qin et al., 2010). Since 2007, Chinese central and local government have implemented a wide range of measures and

management practices for reducing external nutrient inputs, and thus nearly half of external nutrient loads were reduced between 2007 and 2015 (Dai et al., 2016). Nevertheless, every year cyanobacteria bloom still emerge in Taihu Lake up to now, which should be related to internal releases of nutrient loads. It is of great significance to reveal the periodic variations of internal P cycles in Taihu Lake during the algae bloom period and algae collapse period.

In this study, Meiliang bay, a eutrophic and cyanobacteria-dominant zone of Taihu lake, was selected to study the periodic variations and mechanisms of P migration and transformation in aquatic environments during the algae bloom and algae collapse periods. P forms in the water and sediments were determined to characterize the periodic variations of P over the two periods. The *in situ* sampling techniques of diffusive gradients in thin films (DGT) and high-resolution dialysis (HR-Peeper) were used to obtain the information of PO_4^{3-} , ferrous iron (Fe^{2+}) and sulfate (S^{2-}) in the vertical profiles of sediments and pore water. Bacterial community structure in the surface sediments was measured by using 16S rRNA high through sequencing. The aims are to: 1) examine the effect of algae bloom events on the periodic variations of P forms in the water, sediment and pore water; 2) reveal the mechanisms of P migration and transformation over the two periods based on the variations of P forms and bacteria community structures. These results will facilitate lake eutrophication management and algae bloom prevention.

2 Materials and methods

2.1 Study area and sampling

Meiliang bay is in the northern area of Taihu lake, a cyanobacteria-dominant area. In June and December 2021, ten sites in Meiliang bay were selected to collect water samples with the water depths of .5, 1.5, and 2.0 m, as shown in Figure 1. At site-1 of Meiliang bay, three parallel samples of surface sediments and sediment cores were obtained by columnar sediment sampling. A small parts of surface sediments in each sample were stored in a sterile centrifuge tube on-site with dry ice for bacteria community analysis, and other sediments were brought back to the laboratory within 12 h.

2.2 Chemical analysis methods

The pH, dissolved oxygen (DO) and water temperature were measured by a water quality meter (Alalis PD320) on site. In the laboratory, Chlorophyll-a (Chla) content in the water sample was determined by using the spectrophotometry method (Editorial board of Water and Wastewater Monitoring and Analysis Methods, 2002). The original water sample and filtered water sample through fiber filter membrane (pore size of .45 μm) were digested with potassium persulfate solution at 120°C, .1 MPa, and then were used to determine total P (TP) and total dissolved P (TDP) through molybdenum blue method, respectively (Editorial board of Water and Wastewater Monitoring and Analysis Methods, 2002). The orthophosphate (PO_4^{3-}) in the filtered water sample was also determined by using the molybdenum blue method. For each of the water samples, the concentration of TP minus TDP was total particulate P (TPP), and the concentration of TDP minus PO_4^{3-} was dissolved organic P (DOP).

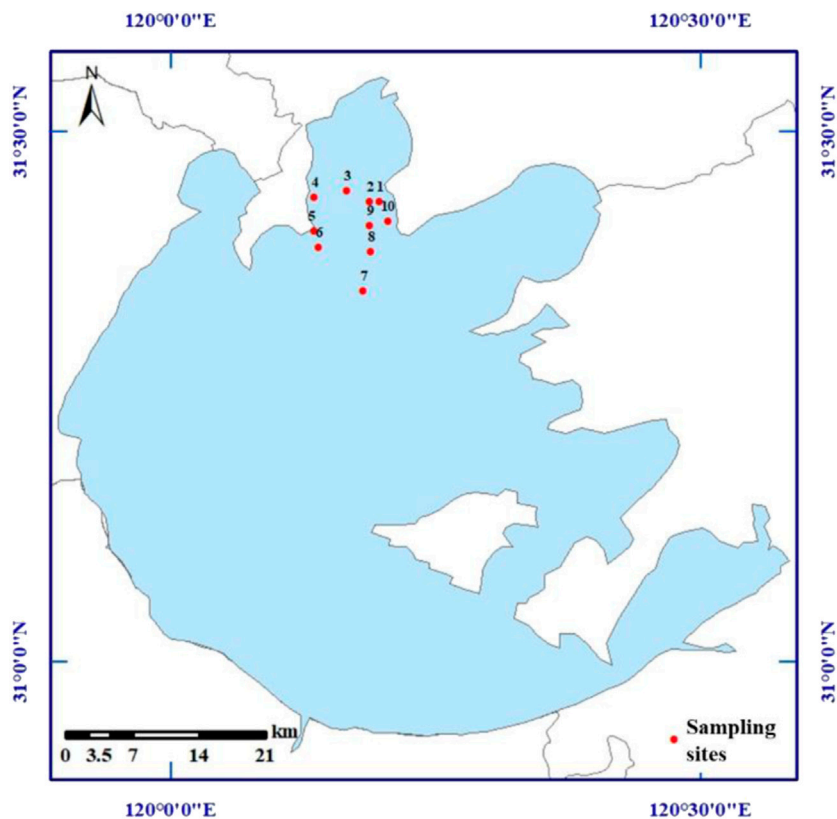


FIGURE 1
Location of sampling sites in Meiliang bay of Taihu Lake in China.

Surface sediment samples were air-dried, ground and sieved by screen mesh with a pore size of .15 mm. The SMT protocol (Ruban et al., 1999) was used to measure sediment P forms, which were divided into soil total P (S-TP), inorganic P (IP), organic P (OP), iron-bound P (FeP) and calcium-bound P (CaP).

2.3 Application of DGT and HR-Peeper techniques

DGT is an *in situ* technique for kinetic passive sampling measurement of analytes in sediments or wet soils over the deployment period (Davison and Zhang, 1994; Krom et al., 2002). In this study, the concentrations of labile PO_4^{3-} , Fe^{2+} and S^{2-} in the sediment cores were simultaneously determined using the DGT technique at depths of -110–10 mm with a vertical resolution of 2.0 mm. The ZrO-Chelex DGT probe was applied for the simultaneous measurements of labile PO_4^{3-} and Fe^{2+} , and the AgI DGT probe was applied for the measurement of labile S^{2-} .

HR-Peeper is an *in situ* sampling technique for analytes in the pore water based on the theory of diffusion equilibrium of ion concentration (Ding et al., 2010). HR-Peeper technique was used to determine concentrations of dissolve PO_4^{3-} and Fe^{2+} in the pore water at depths of -135–15 mm with a vertical resolution of 4.0 mm. These DGT and HR-Peeper probes were provided by Easysensor Co. In China (www.easysensor.net), and the details for their preparations and

assemblies can be seen from previous studies (Xu et al., 2012; Xu et al., 2013).

All of the DGT and HR-Peeper probes were deoxygenated overnight with nitrogen flushing. When the sediments cores at site-1 were delivered to the laboratory, first the HR-Peeper probe was inserted into each of the sediment cores, after 24 h the ZrO-Chelex and AgI DGT probes were also inserted into the same sediment core, and at another 24 h all these probes were carefully retrieved from the sediment core and wiped clean thoroughly using lens wiping paper (Xu et al., 2012).

After being disassembled, the ZrO-Chelex binding gel was sliced at a 2 mm interval using a multi-blade ceramic cutter. Each of the sliced gel pieces was extracted using 1 mol/L HNO_3 for elution of Fe^{2+} , and then was extracted using 1 mol/L NaOH for elution of PO_4^{3-} . The concentrations of the extracted PO_4^{3-} and Fe^{2+} were detected using the molybdenum blue and phenanthroline colorimetric methods, based on which labile PO_4^{3-} and Fe^{2+} concentrations in the sediment cores can be calculated (Xu et al., 2013; Wang et al., 2017). The S^{2-} reacted in the AgI binding gel was measured by the computer imaging densitometry technique, which was used to calculate labile S^{2-} concentrations in the sediment cores (Ding et al., 2012).

After being disassembled, about 200 μL pore water sample was immediately sampled from each chamber of the HR-Peeper probe, and then the concentrations of PO_4^{3-} and Fe^{2+} in the pore water were determined by using the molybdenum blue and phenanthroline colorimetric methods (Ding et al., 2010; Xu et al., 2013), respectively.

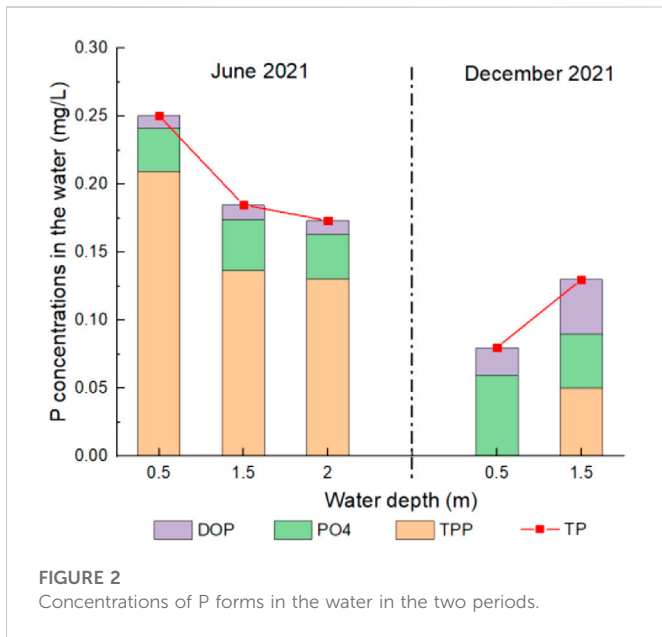


FIGURE 2 Concentrations of P forms in the water in the two periods.

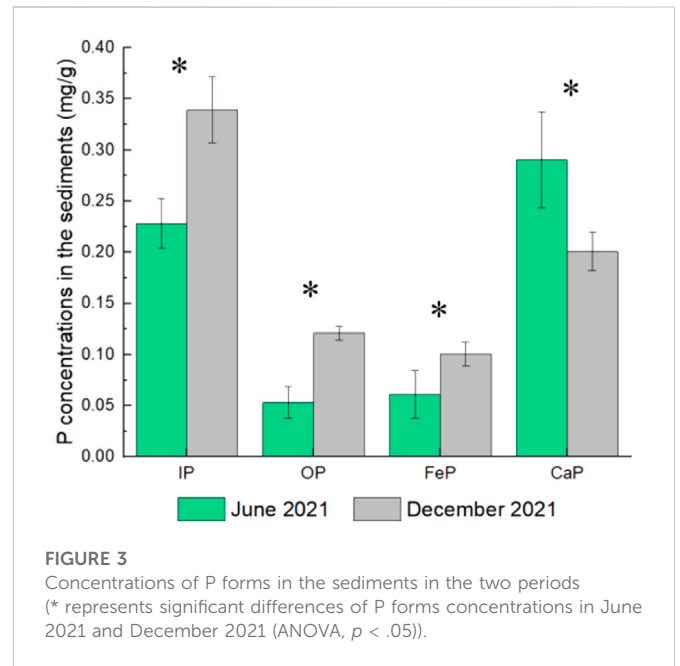


FIGURE 3 Concentrations of P forms in the sediments in the two periods (* represents significant differences of P forms concentrations in June 2021 and December 2021 (ANOVA, $p < .05$)).

2.4 DNA extraction and 16S rRNA gene high throughput sequencing

Total DNA was extracted from .5 g freeze-dried surface sediment sample by E.Z.N.A.® soil DNA spin kit (Omega Bio-tek, Norcross, GA, United.States). The primers set 338F (5'-ACTCCTACGGGA GGCAGCAG-3') and 806R (5'-GGACTACHVGGGTWCTAAT-3') were used in the PCR amplification for targeting the V3~V4 region of bacteria 16S ribosomal RNA gene. PCR product was purified and quantified, sequencing was performed on an Illumina MiSeq PE300 platform (Majorbio Bio-Pharm Technology Co., Ltd., Shanghai, China) according to the standard protocols (<https://cloud.majorbio.com/>).

2.5 Calculations

The diversity of the bacteria community was investigated using the Mothur software, which was displayed as the indices of Shannon, Simpson, ACE, Chao, and Coverage. The heat map of the bacterial community structure was made through the Origin software. The Pearson correlation analysis was performed using the SPSS software.

Based on the concentrations of PO_4^{3-} or Fe^{2+} in the pore water determined by the HR-Peeper technique, the apparent diffusion flux (F_d) of PO_4^{3-} or Fe^{2+} across the interface between pore water and overlying water (the P-O interface) was estimated using the following equations (Fan et al., 2018). ϕ was the sediment porosity (Harper et al., 1998), D_0 was the diffusion coefficient of PO_4^{3-} or Fe^{2+} in the water ($10^{-6} \text{ cm}^2/\text{s}$) (Li and Gregory, 1974), θ was the sediment tortuosity calculated by ϕ , C was the solute concentration of PO_4^{3-} or Fe^{2+} measured by the HR-Peeper probe (mg/L), x is the sediment depth (m), $\frac{\partial C}{\partial x}$ was the concentration gradient of PO_4^{3-} or Fe^{2+} in the pore water core at depths of -20–5 mm (from pore water to overlying water).

$$F_d = -\frac{\phi \cdot D_0}{\theta^2} \frac{\partial C}{\partial x} \quad (1)$$

$$\theta^2 = 1 - \ln(\phi^2) \quad (2)$$

3 Results

3.1 Water quality parameters in the water in the two periods

Water quality parameters including pH, DO, temperature and Chla in Meiliang bay in June and December 2021 are shown in Supplementary Table S1 and Supplementary Figure S1. From June to December, water temperature in the water of Meiliang bay decreased from 26°C to 10°C, and DO contents increased from 6.63 mg/L to 11.25 mg/L, because the low temperature can promote oxygen solubility in the water (Zaker, 2007). The pH values in the water of Meiliang bay varied little between the two periods.

During the sampling period of June 2021, dense blue-green algae were obviously observed on the surface water in Meiliang bay (Supplementary Figure S2). In June 2021, the average content of Chla reached 103.17 $\mu\text{g/L}$ in the surface water, which decreased rapidly as the water depth deepened. In December 2021, Chla contents were stabilized at 22–26 $\mu\text{g/L}$ in the vertical direction of the water.

3.2 P forms in the water and sediments in the two periods

Concentrations of P forms containing PO_4^{3-} , DOP, TPP and TP in the water of Meiliang bay during the two periods are shown in Figure 2. TP and TPP concentrations in the water in June 2021 (.13–.25 mg/L) were much higher than those in December 2021 (0–.13 mg/L), while concentrations of dissolved P contained PO_4^{3-} and DOP were lower than those in December 2021. TPP was the predominant P form in the water in June 2021 which occupied 74%–

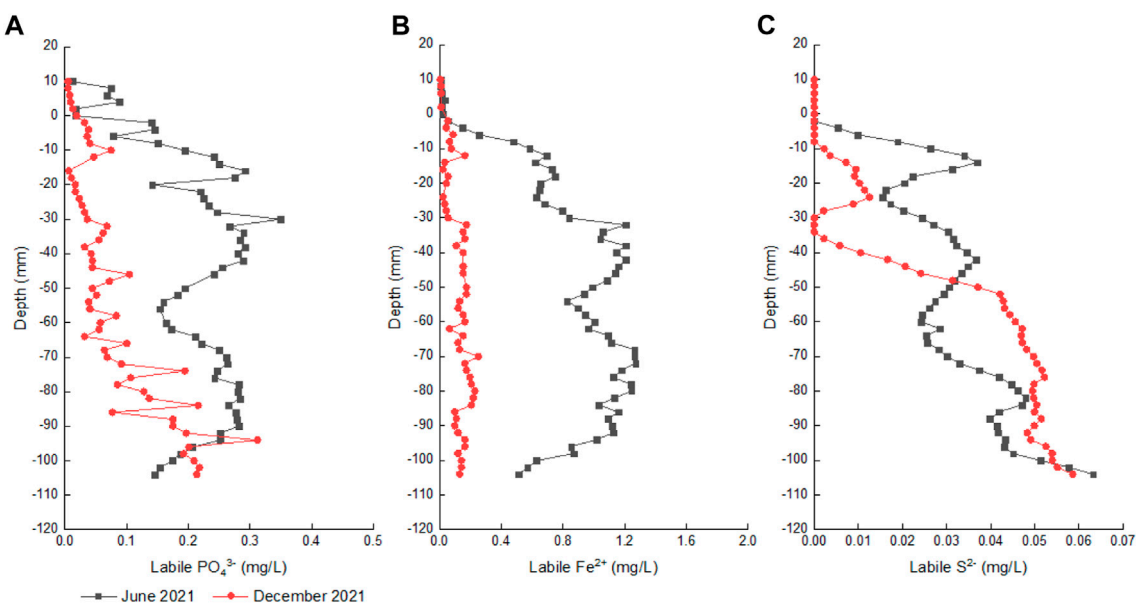


FIGURE 4

Concentrations of labile PO_4^{3-} , Fe^{2+} and S^{2-} in the sediment cores in the two periods. (A–C) represent labile PO_4^{3-} , Fe^{2+} and S^{2-} , respectively.

84% of TP. Dissolved PO_4^{3-} and DOP were the predominant P forms in the water in December 2021. Similar to the vertical distribution of Chla contents in June 2021, concentrations of TP and TPP in the water in June 2021 also decreased as the water depth deepened.

Concentrations of P forms containing IP and OP, FeP, and CaP in the sediments of Meiliang bay during the two periods were shown in Figure 3. The temporal variations of IP, OP and FeP forms in the sediments were different from those of TP and TPP forms in the water. Both IP, OP and FeP concentrations in the sediments in June 2021 (.23, .05 and .06 mg/g) were lower than those in December 2021 (.31, .11 and .09 mg/g), while CaP concentrations in June 2021 (.29 mg/g) was higher than that in December 2021 (.18 mg/g).

3.3 High-resolution distribution of labile PO_4^{3-} , Fe^{2+} and S^{2-} in the sediment cores

Concentrations of labile PO_4^{3-} , Fe^{2+} and S^{2-} in the sediment cores at depths of 10–104 mm were determined by DGT probes with the vertical resolution of 2.0 mm (Figure 4). Concentrations of labile PO_4^{3-} , Fe^{2+} and S^{2-} in the sediment cores in June 2021 were .01–.35, .01–1.27 and 0–.06 mg/L, both of which were relatively higher than those in December 2021 (.01–.31, .01–.25 and 0–.06 mg/L).

In June 2021, labile PO_4^{3-} , Fe^{2+} and S^{2-} in the sediment cores had significant correlations (Supplementary Table S2) and similar vertical distributions, presenting first increases at depths of 0–40 mm and then decreases at depths of 40 to 60 mm (Figure 4). In the deeper depth of 60 to 104 mm, labile PO_4^{3-} and Fe^{2+} concentrations in June increased first and then decreased again, but labile S^{2-} in June increased unsteadily as the sediment depth deepened.

In December 2021, there was only a significant correlation between labile PO_4^{3-} and S^{2-} in the sediment cores (Supplementary Table S2). With the deepening of sediment depth from 0 mm to

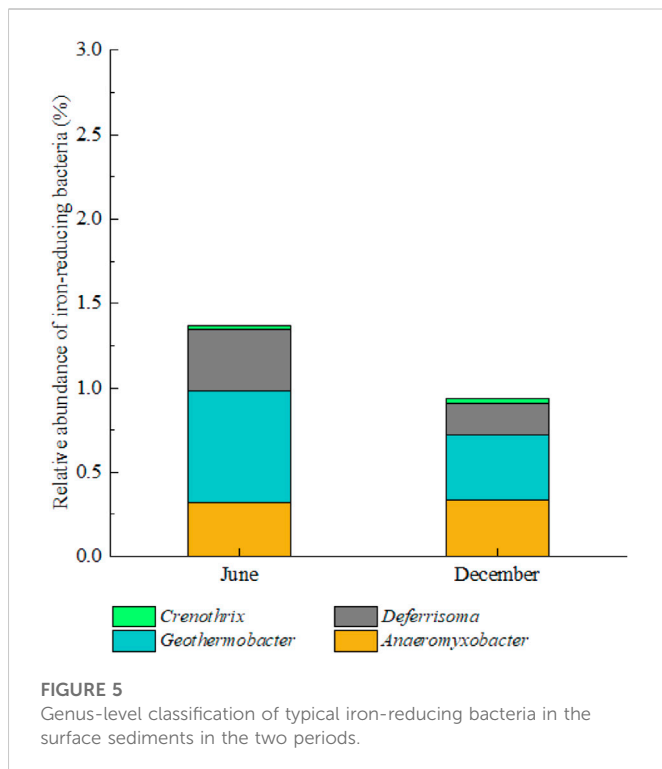
104 mm, labile PO_4^{3-} and S^{2-} concentrations in December exhibited unsteady increases, while labile Fe^{2+} in December increased limitedly.

3.4 High-resolution distribution of PO_4^{3-} and Fe^{2+} in the interface between overlying water and pore water in the two periods

In the pore water and overlying water at depths of 15 to 135 mm, PO_4^{3-} and Fe^{2+} concentrations were determined by HR-Peeper probes with a vertical resolution of 5.0 mm (Supplementary Figure S3). Similar to labile Fe^{2+} in the sediment cores, Fe^{2+} concentrations in the pore water in June (.20–2.03 mg/L) were also higher than that in December (.33–1.16 mg/L). Compared with PO_4^{3-} in the pore water in December 2021, PO_4^{3-} concentrations at depths of 20 to 60 mm were higher but those at depths of 80 to 135 mm were lower in June. In the two periods, both PO_4^{3-} and Fe^{2+} concentrations in the pore water were higher than those in the overlying water, suggesting PO_4^{3-} and Fe^{2+} ions can spontaneously diffuse from pore water to overlying water. The diffusion fluxes of PO_4^{3-} and Fe^{2+} from pore water to overlying water in June (.13 and .33 mg/m²·d) were relatively higher than those in December (.08 and .17 mg/m²·d) (Supplementary Figure S4).

3.5 Bacteria community structure of surface sediments in the two periods

The sequence information calculated the coverage percentage, richness estimator (Chao and ACE), and diversity index (Simpson and Shannon) of the samples in Meiliang bay over the two periods, which were listed in Supplementary Table S3. Based on the ACE and Chao indices, higher bacteria community richness in the surface sediments was found in June 2021. Furthermore, the Simpson and



Shannon indices revealed that the surface sediments in June 2021 had higher bacteria diversity than that in December 2021. There were detected 47 phyla in June and December 2021 with the relative abundance above .01% in the surface sediments of Meiliang bay. [Supplementary Figure S5](#) showed the top thirty phyla. At the phylum level, the dominant bacterial community comprised Proteobacteria (24.63% in June and 22.63% in December), Chloroflexi (13.28% and 12.12%), Acidobacteriota (10.53% and 16.80%), Actinobacteriota (8.90% and 9.96%), Desulfobacterota (8.00% and 8.61%), Bacteroidota (6.23% and 3.04%), Nitrospirota (5.93% and 6.08%) and Nitrospinota (2.47% and 2.86%), etc.

Proteobacteria are commonly found in freshwater sediments, and sedimentary degradation and metabolism rely mainly on the Proteobacteria phylum ([Chaudhry et al., 2012](#)). Furthermore, most of organic P-solubilizing bacteria are predominant in Proteobacteria and Actinobacteriota, which primarily participate in OP mineralization in sediments ([Tu et al., 2022](#)). The relative abundance of Proteobacteria and Actinobacteriota in June 2021 (33.53%) was a bit higher than that in December 2021 (32.59%). In addition, the relative abundance of Desulfobacterota was also ahead of the top thirty ranks of phyla in Meiliang bay, suggesting the sediments had a strong ability for sulfate reduction. The relative abundance of Desulfobacterota in December 2021 (8.61%) was higher than that in June 2021 (8.00%).

At the genus level, some typical iron-reducing bacteria (FRB) in the surface sediments of Meiliang bay in the two periods, including *Anaeromyxobacter*, *Geothermobacter*, *Deferrisoma* and *Crenothrix* ([Fan et al., 2018](#)), were also detected in this study. The relative abundances of these typical FRBs are shown in [Figure 5](#). The relative abundance of FRBs in the surface sediments in June 2021 (1.4%) was higher than that in December 2021 (.9%), suggesting the stronger ability for iron oxides reduction in June 2021.

4 Discussion

4.1 Relationship of periodic changes in algae bloom and water P forms

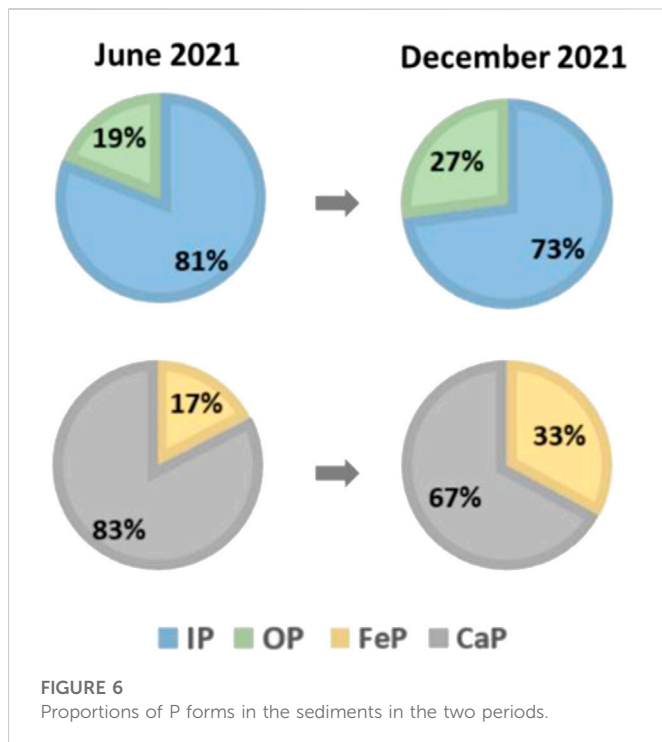
In Taihu Lake, Chla content of 20–40 µg/L had been defined as a threshold of algae blooms, exceeding which was seen as the occurrence of algae bloom ([Xu et al., 2015](#)). In this study, the maximum content of Chla in the surface water of Meiliang bay in June 2021 reached 103.17 µg/L, and it decreased rapidly at the water depths of 1.5 m and 2 m. These reflected the serious state of algae bloom in Meiliang bay in June 2021. Furthermore, algae cells were conditioned to concentrate on the surface water body to compete for sunlight and oxygen ([Huisman et al., 2005](#)). Interestingly, during the sampling period in June 2021, we observed that the concentrated algae cells weren't uniformly flat on the surface water, but presented a lot of strips, as shown in [Supplementary Figure S2](#). In December 2021, Chla contents in the water of Meiliang bay were 22–26 µg/L, so no algae bloom occurred in Meiliang bay during this period. Thus, June 2021 was in the algae bloom period and December 2021 was in the algae collapse period.

The vertical distributions of TP and TPP concentrations in the water of Meiliang bay in June 2021 were similar to Chla, both of which showed extremely higher concentration levels in the surface water. Whereas, in December 2021, there was little TPP in the surface water with the limited algae biomass. A statistical study, covering data from 1992 to 2012, also indicated that annual mean TP concentrations were significantly correlated to Chla contents in Taihu Lake ([Xu et al., 2017](#)). In addition, it had indicated that P form composition in the water body was greatly controlled by the distribution of suspended sands for their strong abilities for P adsorption ([Yao Q. Z. et al., 2016](#); [King et al., 2022](#)). In the algae bloom period (June 2021), the elevated TPP and TP concentrations in the water of Meiliang bay seemed to be not contributed by sand-adsorbing P but intracellular P in the algae cells.

Cyanobacteria is a kind of ancient bacteria with a strong ability for P absorption ([Jeppesen et al., 2005](#)). In the processes of algae growth and reproduction, amounts of PO_4^{3-} are assimilated into algae cells, deriving the transformation of dissolve P to particulate P in the water. When PO_4^{3-} loads in the water were not sufficient to supply algae growth, algae cells can even utilize the products of DOP enzymolysis as their nutritional source ([Ni et al., 2022](#)). Accordingly, dissolved PO_4^{3-} and DOP concentrations in the water of Meiliang bay in June 2021 were much lower than those in December 2021. Therefore, algae appearing and subsiding in the water strongly regulated form composition of dissolved P and particulate P in the water over the different periods. Furthermore, it was implied that algae vertical motion and algae horizontal banding aggregation during the algae bloom period can make spatial heterogeneity of TPP and TP distribution in the water.

4.2 Predominant P forms accumulated in the sediments during the algae collapse period

In contrast to the periodic variations of TPP and TP in the water, sediment P forms such as IP, OP and FeP concentrations in December 2021 (the algae collapse period) were higher than those in June 2021 (the algae bloom period). ([Ding et al., 2018](#)) observed a similar



phenomenon that sediment TP concentrations during the algae collapse period were relatively higher than those during the algae bloom period in Taihu Lake. Thus, during the algae collapse period, the accumulated P forms in the sediments were dominant in OP and FeP, as well as IP since most FeP was included in the IP (Tu et al., 2022).

From the algae bloom period to the algae collapse period, sediment OP accumulation occurred first due to the deposition of dead algae cells accompanied by the migration of algae intracellular P from water to sediments (Kristensen, 1994; Zhang et al., 2021). These biogenic sediments were abundant in organic matter, resulting in the initial OP accumulation in the sediments. It can be verified by the periodic variation of OP proportion in the sediment P of Meiliang bay, which rose from 19% in June 2021 to 27% in December 2021 (Figure 6).

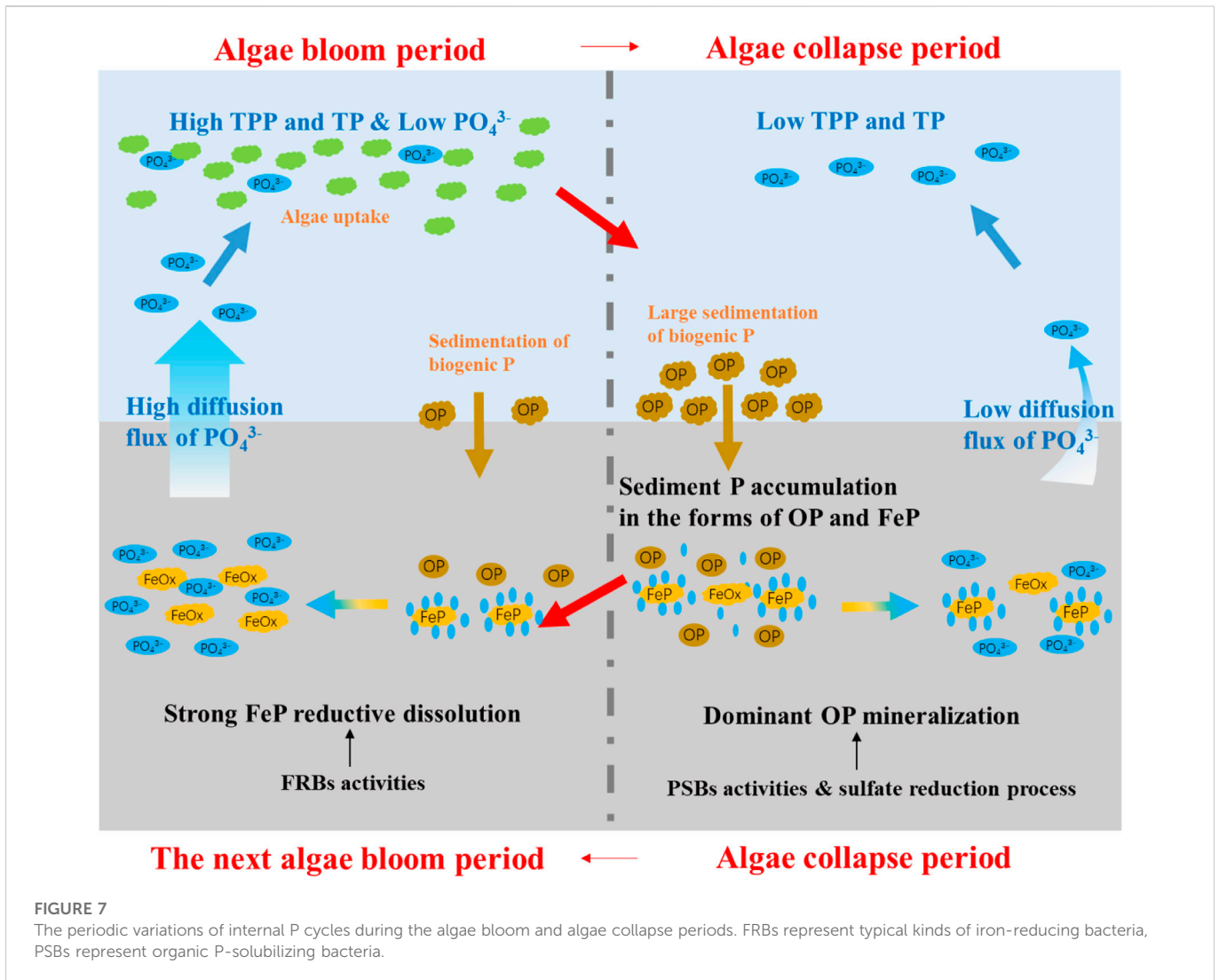
After that sediments have undergone the processes of OP mineralization and FeP formation during the algae collapse period. The proportion of FeP in the sediment P of Meiliang bay in December 2021 (33%) was about 2 times to that in June 2021 (17%) (Figure 6). The increase of FeP proportion in the sediments in December 2021 was unlikely to directly source from the deposition of algae intracellular P, because algae intracellular P was dominant in the form of OP (Kristensen, 1994; Zhang et al., 2021). The increase of FeP proportion in the sediment in December 2021 might be formed through the dissolved PO_4^{3-} adsorption by iron oxides/hydroxides. There were large abundances of Proteobacteria and Actinobacteriota in the sediments of Meiliang bay (Supplementary Figure S5), which contained many kinds of organic P-solubilizing bacteria. Proteobacteria and Actinobacteriota in the sediments would accelerate the conversion of OP into soluble inorganic P (Tu et al., 2022). Then, the released soluble inorganic can be adsorbed onto iron oxides/hydroxides in the sediments (Wang et al., 2019), thus FeP was formed and accumulated in the sediments during the algae collapse period.

4.3 Sediment P regeneration patterns in the algae bloom and collapse periods

Besides sediment P accumulation in December 2021, sediment P release also occurred in Meiliang bay for the positive diffusion fluxes of PO_4^{3-} from pore water to overlying water. However, the diffusion flux of PO_4^{3-} in December 2021 was lower than that in June 2021 (Supplementary Figure S4), suggesting sediment P release was relatively weaker during the algae collapse period than that during the algae bloom period. Both OP mineralization and iron redox cycling are recognized as the main factors controlling P regeneration in the sediments (Ni et al., 2022; Xiao et al., 2022). In the surface sediments of Meiliang bay over the two periods, Proteobacteria and Actinobacteriota occupied above 30% of bacterial community composition, which played important roles in sediment degradation and metabolism, as well as OP mineralization. FeP in the sediments was easily reduced under anaerobic-reductive conditions or by FRBs activities, resulting in the co-release of Fe^{2+} and PO_4^{3-} (Fan et al., 2018). Due to the occurrence of FeP reductive dissolution in the sediments, significant correlations between PO_4^{3-} and Fe^{2+} were often observed in the sediments and pore water of lakes, rivers and oceans (Yao Y. et al., 2016; Sun et al., 2016; Sun et al., 2017; Pan et al., 2019).

During the algae collapse period (December 2021), labile PO_4^{3-} concentrations were not correlated with labile Fe^{2+} but correlated with labile S^{2-} in the sediment cores of Meiliang bay (Supplementary Table S2), and the vertical distribution of PO_4^{3-} was also different from Fe^{2+} in the pore water (Supplementary Figure S3). Thus, FeP reductive dissolution wasn't the main cause of sediment P regeneration in Meiliang bay during the algae collapse period. OP mineralization driven by organic P-solubilizing bacteria activities (Proteobacteria and Actinobacteriota) should predominate sediment P regeneration during the algae collapse period. In addition, concentrations of labile PO_4^{3-} and labile S^{2-} in the sediment cores of Meiliang bay in December 2021 were significantly correlated (Supplementary Table S2), both of which unsteadily increased as the sediment depth deepened (Figure 4). The previous study indicated that rich organic matter (OM) can fuel sulfate reduction under anaerobic sediment conditions (Ma et al., 2017). Usually, active sulfate reduction fueled by OM prevails in the deep sediment zones where oxygen has been depleted (Burdige, 2006). Desulfobacterota works for sulfate reduction in sediments (Fan et al., 2018). The relative abundance of Desulfobacterota in the sediments of Meiliang bay in December 2021 (8.61%) was higher than that in June 2021 (8.00%). Thus, it was inferred that sulfate reduction accompanied by OM degradation might also accelerate the conversion of OP into soluble inorganic P in the sediments during the algae collapse period. Overall, during the algae collapse period, sediment P regeneration in Meiliang bay was mainly attributed to the OP mineralization process driven by organic P-solubilizing bacteria activities and accelerated by the sulfate reduction process.

During the algae bloom period (June 2021), the larger diffusion flux of PO_4^{3-} from pore water to overlying water, as well as the larger Fe^{2+} diffusion flux, can be attributed to FeP reductive dissolution in the sediments. It can be confirmed by the significant correlation between labile PO_4^{3-} and labile Fe^{2+} in the sediments and their similar vertical distributions in June 2021 (Supplementary Table S2; Figure 4). The active area of FeP reductive dissolution in the sediments of Meiliang



bay in June 2021 was concentrated at the sediment depths ranging from -15 mm to -90 mm. Generally, either the reducing environment conditions can drive chemical iron reduction (CIR), or microbe-mediated activities can drive microbial iron reduction (MIR) (Ma et al., 2017). The previous studies indicated that the high electrical conductivity above 300 mV in the upper 35 mm surface sediment layer in Taihu Lake may exclude the CIR process (Christophoridis and Fytianos, 2006; Ding et al., 2018). We observed that the relative abundance of typical FRBs in the sediments of Meiliang bay in June 2021 was higher than that in December 2021 (Figure 5), reflecting the stronger FeP reductive dissolution through MIR during the algae bloom period. Moreover, the promotion of FeP reductive dissolution by FRBs activities may lead to the relatively lower concentrations of FeP and OP in the sediment in June 2021 (Figure 3). In addition, the release and diffusion of PO_4^{3-} through sediment FeP reductive dissolution may also trigger the appearance of algae bloom due to energy saving (Ding et al., 2018). Therefore, although PO_4^{3-} in the surface water was lower in June 2021 (Figure 2), it should be believed that large PO_4^{3-} diffused from pore water to overlying water can be quickly absorbed by algae again in terms of high PO_4^{3-} in the pore water and high TPP in the surface

water during the algae bloom period (Figure 2; Supplementary Figure S4).

4.4 Environment implication

Cutting off loads of exogenous P input and internal P release to eliminate algae bloom events in the eutrophic lakes have been expected (Glibert and Burford, 2017), but there have been greatly underestimated the self-living cycles of P in aquatic environments driven by the processes of algae bloom and algae collapse. This study obtained direct evidence to illustrate the periodic variations of P migration and transformation in Meiliang bay of Taihu Lake, the eutrophic and cyanobacteria-dominant area, which was shown in Figure 7.

During the algae bloom period, the main route of P migration was from sediment P to water P: abundant PO_4^{3-} released from sediments by FeP reductive dissolution were migrated upward and then transported into algae cells by algae uptake of PO_4^{3-} , being TPP form in the surface water. Whereas, P migration from water to sediment was dominant in the algae collapse period, during which

sediment P was mainly accumulated in the forms of OP and FeP. In the algae collapse period, the early formed TPP due to algae bloom settled in the sediments resulting in OP accumulation at first, and then sediment FeP was formed and accumulated through the processes of OP mineralization and P adsorption of iron oxides/hydroxides. Furthermore, the PO_4^{3-} existed in the pore water and PO_4^{3-} released from pore water to overlying water in Meiliang bay were based on the different sediment P regeneration routes in the two periods. During the algae bloom period, FeP reductive dissolution driven by FRBs activities was the main factor responsible for the dissolution and release of PO_4^{3-} in the sediments. Sediment P regeneration during the algae collapse period was mainly attributed to the OP mineralization process driven by organic P-solubilizing bacteria activities and accelerated by the sulfate reduction process.

A lack of understanding of the periodic variations of P migration and transformation patterns in aquatic environments with frequent algae bloom events can lead to inefficient treatments of lake eutrophication and algae bloom. For instance, the flocculation of algae cells using modified local soils, sands or bio modified activated carbon can rapidly make cyanobacteria or *Microcystis* cells disappear during the algae bloom period (Shi et al., 2016; Wang et al., 2016), but they just accomplish sediment P accumulation several months ahead of the algae collapse period, and they cannot prevent the development of the next algae bloom because of sediment P regeneration. Accordingly, it is best to implement capping and stabilization of treatments for sediment P (Douglas et al., 2016; Gu B.-W. et al., 2019) after the algae collapse period and before the next algae bloom period. Therefore, for eutrophic lakes, treatment approaches and management practices require special consideration about how to break the self-living cycles of P in aquatic environments driven by algae bloom and algae collapse processes.

5 Conclusion

This study obtained direct evidence to illustrate the periodic variations of P migration and transformation patterns in the Meiliang bay of Taihu Lake during the algae bloom and algae collapse periods. Due to the uptake of PO_4^{3-} by algae, high concentrations of TPP and TP in the surface water were characterized during the algae bloom period. Furthermore, the sediment layer had higher internal P diffusion fluxes during the algae bloom period than those during the algae collapse period. These were mainly attributed to the occurrence of FeP reductive dissolution by FRBs activities, resulting in the relatively low concentrations and proportions of FeP in the sediments during the algae bloom period.

During the algae collapse period, the relatively high concentrations of OP and FeP in the surface sediments were observed, suggesting the dominant migration route of P from water to sediments. Moreover, FeP was formed and accumulated in the sediments through the processes of OP mineralization and P adsorption of iron oxides/hydroxides during the algae collapse period. Sediment P was still being released during the algae

collapse period, which was caused by the OP mineralization process driven by organic P-solubilizing bacteria activities and accelerated by the sulfate reduction process. The different patterns of P migration and transformation in aquatic environments during the algae bloom and algae collapse periods were expected to provide theoretical support for the prevention and control of lake water eutrophication and algae bloom events.

Data availability statement

The original contributions presented in the study are included in the article/[Supplementary Material](#), further inquiries can be directed to the corresponding author.

Author contributions

Conceptualization is contributed by CH; investigation is contributed by YT, HW, NS, and YD; data curation is contributed by YT, HW and NS; formal analysis is contributed by YD and TD; writing—original draft preparation is contributed by CH; writing—review and editing is contributed by CH, YT and HW.

Funding

The work was financially supported by Natural Science Foundation of Jiangsu province in China (No. BK20190763) and National Natural Science Foundation of China (No. 42007346).

Conflict of interest

The authors declare that the research was conducted in the absence of any commercial or financial relationships that could be construed as a potential conflict of interest.

The reviewer ZW declared a shared affiliation with the authors to the handling editor at time of review.

Publisher's note

All claims expressed in this article are solely those of the authors and do not necessarily represent those of their affiliated organizations, or those of the publisher, the editors and the reviewers. Any product that may be evaluated in this article, or claim that may be made by its manufacturer, is not guaranteed or endorsed by the publisher.

Supplementary material

The Supplementary Material for this article can be found online at: <https://www.frontiersin.org/articles/10.3389/feart.2022.1097679/full#supplementary-material>

References

- Burdige, D. J. (2006). *Geochemistry of marine sediments*. Princeton, NY, USA: Princeton University Press.
- Chaudhry, V., Rehman, A., Mishra, A., Chauhan, P. S., and Nautiyal, C. S. (2012). Changes in bacterial community structure of agricultural land due to long-term organic and chemical amendments. *Microb. Ecol.* 64, 450–460. doi:10.1007/s00248-012-0025-y
- Chen, M., Ding, S., Chen, X., Sun, Q., Fan, X., Lin, J., et al. (2018). Mechanisms driving phosphorus release during algal blooms based on hourly changes in iron and phosphorus concentrations in sediments. *Water Res.* 133, 153–164. doi:10.1016/j.watres.2018.01.040
- Chen, M., Ding, S., Liu, L., Xu, D., Han, C., and Zhang, C. (2015). Iron-coupled inactivation of phosphorus in sediments by macrozoobenthos (chironomid larvae) bioturbation: Evidences from high-resolution dynamic measurements. *Environ. Pollut.* 204, 241–247. doi:10.1016/j.envpol.2015.04.031
- Christophoridis, C., and Fytianos, K. (2006). Conditions affecting the release of phosphorus from surface lake sediments. *J. Environ. Qual.* 35, 1181–1192. doi:10.2134/jeq2005.0213
- Dai, X. L., Qian, P. Q., Ye, L., Song, T., and Ting, S. (2016). Changes in nitrogen and phosphorus concentrations in Lake Taihu, 1985–2015. *J. Lake Sci.* 28, 935–943. (in Chinese). doi:10.18307/2016.0502
- Davison, W., and Zhang, H. (1994). *In situ* speciation measurements of trace components in natural waters using thin-film gels. *Nature* 367, 546–548. doi:10.1038/367546a0
- Ding, S. M., Chen, M. S., Gong, M. D., Fan, X. F., Qin, B. Q., Xu, H., et al. (2018). Internal phosphorus loading from sediments causes seasonal nitrogen limitation for harmful algal blooms. *Sci. Total Environ.* 625, 872–884. doi:10.1016/j.scitotenv.2017.12.348
- Ding, S. M., Sun, Q., and Xu, D. (2010). Development of the DET technique for high-resolution determination of soluble reactive phosphate profiles in sediment pore waters. *Int. J. Environ. Anal. Chem.* 90, 1130–1138. doi:10.1080/03067310903434733
- Ding, S. M., Sun, Q., Xu, D., Jia, F., He, X., and Zhang, C. (2012). High-resolution simultaneous measurements of dissolved reactive phosphorus and dissolved sulfide: The first observation of their simultaneous release in sediments. *Environ. Sci. Technol.* 46, 8297–8304. doi:10.1021/es301134h
- Douglas, G. B., Lurling, M., and Spears, B. M. (2016). Assessment of changes in potential nutrient limitation in an impounded river after application of lanthanum-modified bentonite. *Water Res.* 97, 47–54. doi:10.1016/j.watres.2016.02.005
- Editorial board of Water and Wastewater Monitoring and Analysis Methods (2002). *Water and wastewater monitoring and analysis methods*. Tsing Hua, China: China Environmental Science Press, 670–671. (in Chinese).
- Fan, X. F., Ding, S. M., Gong, M. D., Chen, M. S., Gao, S. S., Jin, Z. F., et al. (2018). Different influences of bacterial communities on Fe (III) reduction and phosphorus availability in sediments of the cyanobacteria- and macrophyte-dominated zones. *Front. Microbiol.* 9, 2636. doi:10.3389/fmicb.2018.02636
- Gao, Y. L., Liang, T., Tian, S. H., Wang, L., Holm, P. E., and C. B. H. H. (2016). High-resolution imaging of labile phosphorus and its relationship with iron redox state in lake sediments. *Environ. Pollut.* 219, 466–474. doi:10.1016/j.envpol.2016.05.053
- Gilbert, P. M. (2017). Eutrophication, harmful algae and biodiversity - challenging paradigms in a world of complex nutrient changes. *Mar. Pollut. Bull.* 124, 591–606. doi:10.1016/j.marpolbul.2017.04.027
- Gilbert, P. M., and Burford, M. A. (2017). Globally changing nutrient loads and harmful algal blooms recent advances, new paradigms, and continuing challenges. *Oceanography* 30, 58–69. doi:10.5670/oceanog.2017.110
- Gu, B.-W., Hong, S.-H., Lee, C.-G., and Park, S.-J. (2019a). The feasibility of using bentonite, illite, and zeolite as capping materials to stabilize nutrients and interrupt their release from contaminated lake sediments. *Chemosphere* 219, 217–226. doi:10.1016/j.chemosphere.2018.12.021
- Gu, S., Gruau, G., Dupas, R., Petitjean, P., Li, Q., and Pinay, G. (2019b). Respective roles of Fe-oxhydroxide dissolution, pH changes and sediment inputs in dissolved phosphorus release from wetland soils under anoxic conditions. *Geoderma* 338, 365–374. doi:10.1016/j.geoderma.2018.12.034
- Han, C., Ding, S. M., Yao, L., Shen, Q. S., Zhu, C. G., Wang, Y., et al. (2015). Dynamics of phosphorus-iron-sulfur at the sediment-water interface influenced by algae blooms decomposition. *J. Hazard. Mater.* 300, 329–337. doi:10.1016/j.jhazmat.2015.07.009
- Harper, M. P., Davison, W., Zhang, H., and Tych, W. (1998). Kinetics of metal exchange between solids and solutions in sediments and soils interpreted from DGT measured fluxes. *Geochimica Cosmochimica Acta* 62, 2757–2770. doi:10.1016/s0016-7037(98)00186-0
- Huisman, J., Matthijs, H. C., and Visser, P. M. (2005). *Harmful cyanobacteria*. Dordrecht, Netherlands: Springer.
- Jeppesen, E., Sondergaard, M., Jensen, J. P., Havens, K. E., Anneville, O., Carvalho, L., et al. (2005). Lake responses to reduced nutrient loading - an analysis of contemporary long-term data from 35 case studies. *Freshw. Biol.* 50, 1747–1771. doi:10.1111/j.1365-2427.2005.01415.x
- King, W. M., Curless, S. E., and Hood, J. M. (2022). River phosphorus cycling during high flow may constrain Lake Erie cyanobacteria blooms. *Water Res.* 222, 118845. doi:10.1016/j.watres.2022.118845
- Kouakou, C. R. C., and Poder, T. G. (2019). Economic impact of harmful algal blooms on human health: A systematic review. *J. Water Health* 17, 499–516. doi:10.2166/wh.2019.064
- Kristensen, E. (1994). Decomposition of macroalgae, vascular plants and sediment detritus in seawater: Use of stepwise thermogravimetry. *Biogeochemistry* 26, 1–24. doi:10.1007/BF02180401
- Krom, M. D., Mortimer, R. J. G., Poulton, S. W., Hayes, P., Davies, I. M., Davison, W., et al. (2002). *In-situ* determination of dissolved iron production in recent marine sediments. *Aquat. Sci.* 64, 282–291. doi:10.1007/s00027-002-8072-y
- Lepori, F., and Roberts, J. J. (2017). Effects of internal phosphorus loadings and food-web structure on the recovery of a deep lake from eutrophication. *J. Great Lakes Res.* 43, 255–264. doi:10.1016/j.jglr.2017.01.008
- Li, Y. H., and Gregory, S. (1974). Diffusion of ions in sea water and in deep-sea sediments. *Geochimica Cosmochimica Acta* 38, 703–714. doi:10.1016/0016-7037(74)90145-8
- Liu, Y. Q., Cao, X. Y., Li, H., Zhou, Z. J., Wang, S. Y., Wang, Z. C., et al. (2017). Distribution of phosphorus-solubilizing bacteria in relation to fractionation and sorption behaviors of phosphorus in sediment of the Three Gorges Reservoir. *Environ. Sci. Pollut. Res.* 24, 17679–17687. doi:10.1007/s11356-017-9339-0
- Ma, W. W., Zhu, M. X., Yang, G. P., and Li, T. (2017). *In situ*, high-resolution DGT measurements of dissolved sulfide, iron and phosphorus in sediments of the East China Sea: Insights into phosphorus mobilization and microbial iron reduction. *Mar. Pollut. Bull.* 124, 400–410. doi:10.1016/j.marpolbul.2017.07.056
- Ni, Z., Huang, D., Li, Y., Liu, X., and Wang, S. (2022). Novel insights into molecular composition of organic phosphorus in lake sediments. *Water Res.* 214, 118197. doi:10.1016/j.watres.2022.118197
- Pan, F., Liu, H., Guo, Z., Li, Z., Wang, B., Cai, Y., et al. (2019). Effects of tide and season changes on the iron-sulfur-phosphorus biogeochemistry in sediment porewater of a mangrove coast. *J. Hydrology* 568, 686–702. doi:10.1016/j.jhydrol.2018.11.002
- Qian, Y. C., Liang, X. Q., Chen, Y. X., Lou, L. P., Cui, X. Y., Tang, J. E., et al. (2011). Significance of biological effects on phosphorus transformation processes at the water-sediment interface under different environmental conditions. *Ecol. Eng.* 37, 816–825. doi:10.1016/j.ecoleng.2010.12.005
- Qin, B., Zhu, G., Gao, G., Zhang, Y., Li, W., Paerl, H. W., et al. (2010). A drinking water crisis in lake Taihu, China: Linkage to climatic variability and lake management. *Environ. Manag.* 45, 105–112. doi:10.1007/s00267-009-9393-6
- Ruban, V., Lopez-Sanchez, J. F., Pardo, P., Rauret, G., Muntua, H., and Quevauviller, P. (1999). Selection and evaluation of sequential extraction procedures for the determination of phosphorus forms in lake sediment. *J. Environ. Monit.* 1, 51–56. doi:10.1039/a807778i
- Schelske, C. L. (2009). Eutrophication: Focus on phosphorus. *Science* 324, 722. doi:10.1126/science.324.722
- Schindler, D. W., Carpenter, S. R., Chapra, S. C., Hecky, R. E., and Orihel, D. M. (2016). Reducing phosphorus to curb lake eutrophication is a success. *Environ. Sci. Technol.* 50, 8923–8929. doi:10.1021/acs.est.6b02204
- Shi, W. Q., Tan, W. Q., Wang, L. J., and Pan, G. (2016). Removal of *Microcystis aeruginosa* using cationic starch modified soils. *Water Res.* 97, 19–25. doi:10.1016/j.watres.2015.06.029
- Sun, Q. Q., Chen, J. A., Wang, J. F., Yang, H. Q., Ji, Y. X., Lan, C., et al. (2017). [High-resolution distribution characteristics of phosphorus, iron and sulfur across the sediment-water interface of aha reservoir]. *J. Environ. Sci.* 38, 2810–2818. (in Chinese). doi:10.13227/j.hjck.201611159
- Sun, Q., Sheng, Y., Yang, J., Di Bonito, M., and Mortimer, R. J. G. (2016). Dynamic characteristics of sulfur, iron and phosphorus in coastal polluted sediments, north China. *Environ. Pollut.* 219, 588–595. doi:10.1016/j.envpol.2016.06.019
- Tu, C., Jin, Z., Che, F., Cao, X., Song, X., Lu, C., et al. (2022). Characterization of phosphorus sorption and microbial community in lake sediments during overwinter and recruitment periods of cyanobacteria. *Chemosphere* 307, 135777. doi:10.1016/j.chemosphere.2022.135777
- Wang, C., Fang, F., Yuan, Z., Zhang, R., Zhang, W., and Guo, J. (2020). Spatial variations of soil phosphorus forms and the risks of phosphorus release in the water-level fluctuation zone in a tributary of the Three Gorges Reservoir. *Sci. Total Environ.* 699, 134124. doi:10.1016/j.scitotenv.2019.134124
- Wang, L. J., Pan, G., Shi, W. Q., Wang, Z. B., and Zhang, H. G. (2016). Manipulating nutrient limitation using modified local soils: A case study at lake Taihu (China). *Water Res.* 101, 25–35. doi:10.1016/j.watres.2016.05.055
- Wang, Y., Ding, S. M., Shi, L., Gong, M. D., Xu, S. W., and Zhang, C. S. (2017). Simultaneous measurements of cations and anions using diffusive gradients in thin films with a ZrO-Chelex mixed binding layer. *Anal. Chim. Acta* 972, 1–11. doi:10.1016/j.aca.2017.04.007
- Wang, Z., Huang, S., and Li, D. (2019). Decomposition of cyanobacterial bloom contributes to the formation and distribution of iron-bound phosphorus (Fe-P): Insight for cycling mechanism of internal phosphorus loading. *Sci. Total Environ.* 652, 696–708. doi:10.1016/j.scitotenv.2018.10.260
- Xiao, K., Pan, F., Santos, I. R., Zheng, Y., Zheng, C. M., Chen, N. W., et al. (2022). Crab bioturbation drives coupled iron-phosphate-sulfide cycling in mangrove and salt marsh soils. *Geoderma* 424, 115990. doi:10.1016/j.geoderma.2022.115990

- Xu, D., Chen, Y., Ding, S., Sun, Q., Wang, Y., and Zhang, C. (2013). Diffusive gradients in thin films technique equipped with a mixed binding gel for simultaneous measurements of dissolved reactive phosphorus and dissolved iron. *Environ. Sci. Technol.* 47, 10477–10484. doi:10.1021/es401822x
- Xu, D., Wu, W., Ding, S. M., Sun, Q., and Zhang, C. (2012). A high-resolution dialysis technique for rapid determination of dissolved reactive phosphate and ferrous iron in pore water of sediments. *Sci. Total Environ.* 1, 245–252. doi:10.1016/j.scitotenv.2012.01.062
- Xu, H., Paerl, H. W., Qin, B., Zhu, G., Hall, N. S., and Wu, Y. (2015). Determining critical nutrient thresholds needed to control harmful cyanobacterial blooms in eutrophic lake Taihu, China. *Environ. Sci. Technol.* 49, 1051–1059. doi:10.1021/es503744q
- Xu, H., Paerl, H. W., Zhu, G. W., Qin, B. Q., Hall, N. S., and Zhu, M. Y. (2017). Long-term nutrient trends and harmful cyanobacterial bloom potential in hypertrophic Lake Taihu, China. *Hydrobiologia* 787, 229–242. doi:10.1007/s10750-016-2967-4
- Yao, Q. Z., Du, J. T., Chen, H. T., and Yu, Z. G. (2016a). Particle-size distribution and phosphorus forms as a function of hydrological forcing in the Yellow River. *Environ. Sci. Pollut. Res. Int.* 23, 3385–3398. doi:10.1007/s11356-015-5567-3
- Yao, Y., Wang, P. F., Wang, C., Hou, J., Miao, L., Yuan, Y., et al. (2016b). Assessment of mobilization of labile phosphorus and iron across sediment-water interface in a shallow lake (Hongze) based on *in situ* high-resolution measurement. *Environ. Pollut.* 219, 873–882. doi:10.1016/j.envpol.2016.08.054
- Yuan, H., Tai, Z., Li, Q., and Zhang, F. (2020). Characterization and source identification of organic phosphorus in sediments of a hypereutrophic lake. *Environ. Pollut.* 257, 113500. doi:10.1016/j.envpol.2019.113500
- Zaker, N. H. (2007). Characteristics and seasonal variations of dissolved oxygen. *Int. J. Environ. Res.* 1, 296–301. doi:10.22059/IJER.2010.140
- Zhang, L., Huang, S., Peng, X., Liu, B., Zhang, X., Ge, F., et al. (2021). Potential ecological implication of *Cladophora oligoclora* decomposition: Characteristics of nutrient migration, transformation, and response of bacterial community structure. *Water Res.* 190, 116741. doi:10.1016/j.watres.2020.116741
- Zhang, W., Zhu, X., Jin, X., Meng, X., Tang, W., and Shan, B. (2017). Evidence for organic phosphorus activation and transformation at the sediment-water interface during plant debris decomposition. *Sci. Total Environ.* 583, 458–465. doi:10.1016/j.scitotenv.2017.01.103